From single drug targets to synergistic network pharmacology in ischemic stroke

Ana I. Casas[a,1], Ahmed A. Hassan[a], Simon J. Larsen[b], Vanessa Gomez-Rangel[c], Mahmoud Elbatreek[a], Pamela W. M. Kleikers[a], Emre Guney[a,d], Javier Egea[e], Manuela G. López[c], Jan Baumbach[f], and Harald H. H. W. Schmidt[a,1]

[a]Department of Pharmacology and Personalised Medicine, Maastricht Center for Systems Biology, Faculty of Health, Medicine and Life Sciences, Maastricht University, 6229 ER Maastricht, The Netherlands; [b]Computational Biology Lab, Department of Mathematics and Computer Science, University of Southern Denmark, 5230 Odense, Denmark; [c]Instituto Teofilo Hernando, Departamento de Farmacología, Facultad de Medicina, Universidad Autónoma de Madrid, 28029 Madrid, Spain; [d]Research Programme on Biomedical Informatics, The Hospital del Mar Medical Research Institute and Pompeu Fabra University, 08003 Barcelona, Spain; [e]Servicio de Farmacología Clínica, Instituto de Investigación Sanitaria–Hospital Universitario de la Princesa, 28006 Madrid, Spain; and [f]Chair of Experimental Bioinformatics, TUM School of Life Sciences Weihenstephan, Technical University of Munich, 85354 Munich, Germany

Drug discovery faces an efficacy crisis to which ineffective mainly single-target and symptom-based rather than mechanistic approaches have contributed. We here explore a mechanism-based disease definition for network pharmacology. Beginning with a primary causal target, we extend this to a second using guilt-by-association analysis. We then validate our prediction and explore synergy using both cellular in vitro and mouse in vivo models. As a disease model we chose ischemic stroke, one of the highest unmet medical need indications in medicine, and reactive oxygen species forming NADPH oxidase type 4 (Nox4) as a primary causal therapeutic target. For network analysis, we use classical protein–protein interactions but also metabolite-dependent interactions. Based on this protein–metabolite network, we conduct a gene ontology-based semantic similarity ranking to find suitable synergistic cotargets for network pharmacology. We identify the nitric oxide synthase (Nos1 to 3) gene family as the closest target to Nox4. Indeed, when combining a NOS and a NOX inhibitor at subthreshold concentrations, we observe pharmacological synergy as evidenced by reduced cell death, reduced infarct size, stabilized blood–brain barrier, reduced reoxygenation-induced leakage, and preserved neuromotor function, all in a supraadditive manner. Thus, protein–metabolite network analysis, for example guilt by association, can predict and pair synergistic mechanistic disease targets for systems medicine-driven network pharmacology. Such approaches may in the future reduce the risk of failure in single-target and symptom-based drug discovery and therapy.

network pharmacology | stroke | NOX4 | network analysis

In drug discovery, a "one disease–one target–one drug" approach is common practice, primarily to simplify compound screening, reduce unwanted side effects, and simplify registration (1). This approach, however, oversimplifies disease mechanisms, which are in fact complex subnetworks within the interactome (2, 3). Moreover, disease definitions are mostly symptom- rather than mechanism-based, and hence the therapeutics are likewise. Not surprisingly, drug discovery has thus become increasingly inefficient (4). Conversely, systems medicine and network pharmacology define diseases according to causal mechanisms (5, 6). Moreover, network pharmacology aims to further enhance this by targeting not only a single component within such a network but by combining drugs within these networks with the aim of achieving synergy and dose reduction (7). However, most network databases are curated (8); the de novo identification of such networks is only in its beginning. De novo network enrichment from a single primary validated target toward at least one secondary target holds high promise for systems medicine (9) but is currently not possible.

To address this challenge, we designed an approach that (i) is integrative, (ii) is based on the network pharmacology paradigm,

(iii) predicts targets instead of drugs, (iv) is validated through experiment, and (v) is readily applicable by a broad range of biomedical scientists. In fact, our approach can be established as a powerful tool and therefore implemented in novel, complex, and frequently unexpected indications where already-marketed drugs can be repurposed, leading to new therapies. Our strategy amends the limitations of previous approaches, for example, simple pairwise combination of drugs as opposed to targeting networks (10, 11), or combining drugs, which may have different off-target effects, rather than drug targets (10–12). Furthermore, most proposed computational methods have not been validated experimentally for de novo predictions (10–14). Moreover, most of these methods rely on drug similarity signatures extracted from chemical structures, targets, and side effect profiles, introducing a potential bias toward the pharmacological classes currently represented in knowledge bases (15) and limiting their applicability to de novo candidate discovery (16).

Significance

Current one drug–one target–one disease approaches in drug discovery have become increasingly inefficient. Network pharmacology defines disease mechanisms as networks best targeted by multiple, synergistic drugs. Using the high unmet medical need indication stroke, we here develop an integrative in silico approach based on a primary target, NADPH oxidase type 4, to identify a mechanistically related cotarget, NO synthase, for network pharmacology. Indeed, we validate both in vivo and in vitro, including humans, that both NOX4 and NOS inhibition is highly synergistic, leading to a significant reduction of infarct volume, direct neuroprotection, and blood–brain-barrier stabilization. This systems medicine approach provides a ground plan to decrease current failure in the field by being implemented in other complex indications.

PHARMACOLOGY

www.manaraa.com

We therefore here develop a simple and integrative in silico approach to pair an existing validated primary causal therapeutic target with a synergistic cotarget within a network pharmacology strategy. We importantly validate our prediction both in vitro and in vivo, including a suitable in vitro human model. As a disease model for this we chose ischemic stroke, a multifactorial high unmet medical need indication for which no neuroprotective therapy is currently available. As a mechanistic starting point (node), we selected the reactive oxygen-forming enzyme NADPH oxidase type 4 (NOX4), a preclinically highly validated target directly involved in neurotoxicity and poststroke blood–brain barrier dysfunction (17, 18).

Results

Guilt-by-Association Analysis and Network Construction. To identify synergistic and mechanistically related cotargets for NOX4, we employed a guilt-by-association analysis on a multilayered molecular interaction network. Since many signaling events are governed by intermediate metabolites rather than protein–protein interactions (19), we considered this approach alone as insufficient to search for secondary targets. We therefore combined protein–protein interactions with protein–metabolite interactions to overcome such a potential bias or limitation.

We adopted a bottom-up approach consisting of three interacting computational modules starting from a well-known clinical target in stroke, NOX4 (17), as our primary target protein and seed node (Fig. 1). In module 1, we expanded from this seed node to obtain a network of candidate targets and related metabolites, resulting in five metabolites which were extended to their interactors, yielding 537 proteins. The main product of *Nox4* (20), hydrogen peroxide (H_2O_2), and the substrate, oxygen (O_2), were manually added due to their absence from the Human Metabolome Database (HMDB), and a curation request was sent to the database. As a filtering step for narrowing down the interactions search space, drug–target interactions were used, resulting in 166 potential druggable target proteins. In module 2, a protein–protein interaction network was constructed based on the previously obtained druggable target proteins (Fig. 1). Subsequently, networks from modules 1 and 2 were combined to obtain a two-layered network determining the closest interaction partners of our primary target by means of guilt by association (21). Hence, several levels of connectedness to NOX4 were observed, via direct protein interactions or indirect metabolic interactions (Fig. 2A), of which we consider the highest level, including nine proteins, as suitable NOX4-synergistic targets (Table 1). The full list of protein connectedness is reported in *SI Appendix*, Table S2.

Semantic Similarity of Gene Ontology Terms Affirms Network Analysis Results. Semantic similarity quantifies the closeness or relatedness of two strings or terms, in our case the different gene
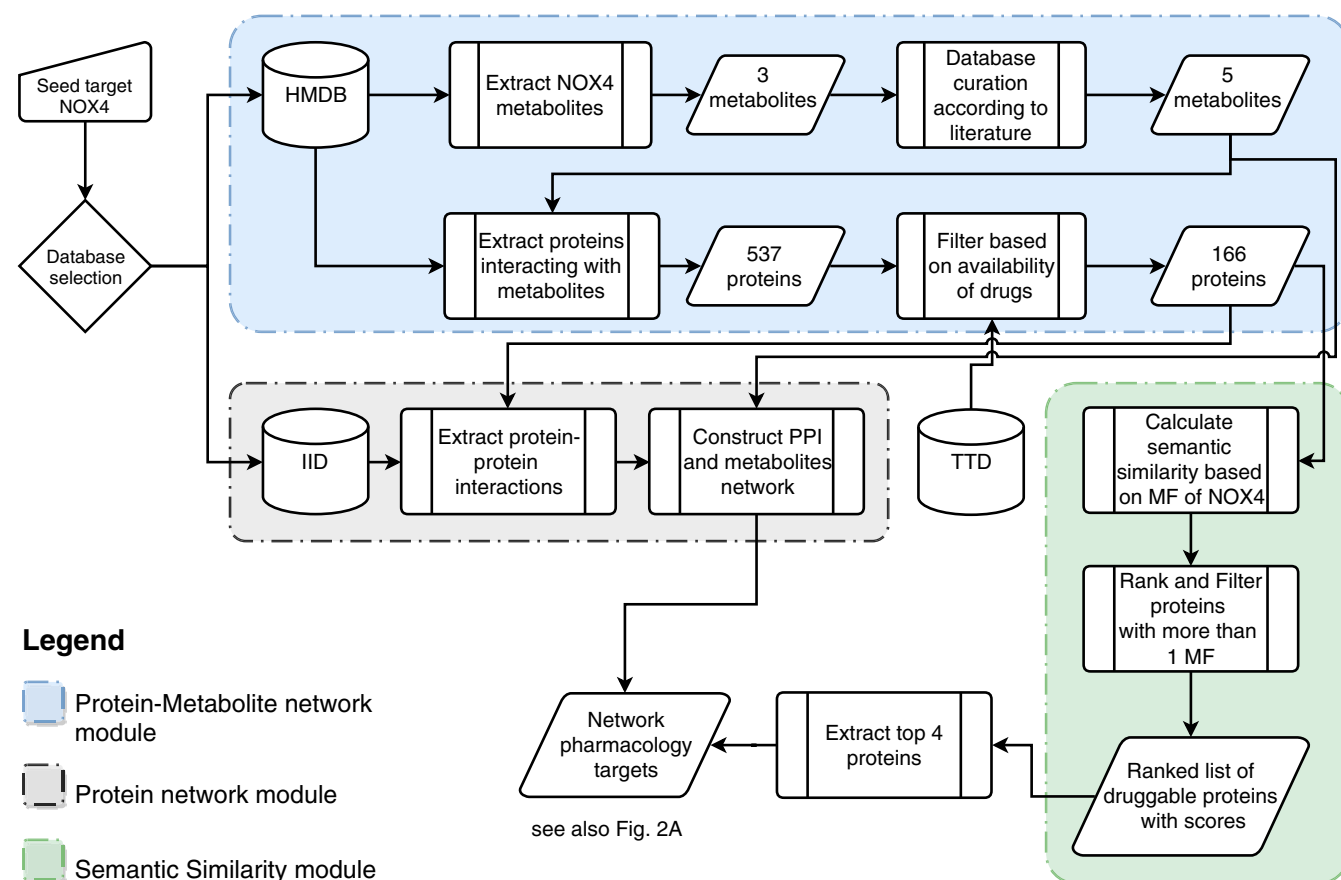

Fig. 1. Computational workflow for target prioritization via network pharmacology. The computational target prioritization pipeline consists of three interdependent modules. The blue module extracts the metabolites interacting with the protein NOX4 from the Human Metabolome Database, performs curation of the metabolites, extracts the proteins interacting with them, and filters them based on the availability of drugs from the Therapeutic Target Database (TTD). The gray module uses the Integrated Interaction Database (IID) to extract protein–protein interactions of the proteins yielded by the blue module and constructs a network out of them. The green module calculates gene ontology-based semantic similarity scores of the output of the blue module compared with NOX4 using molecular function (MF) annotations, ranks the proteins based on their similarity scores, and excludes proteins with less than one molecular function. The output of the green module is used to annotate the network with the top four proteins.
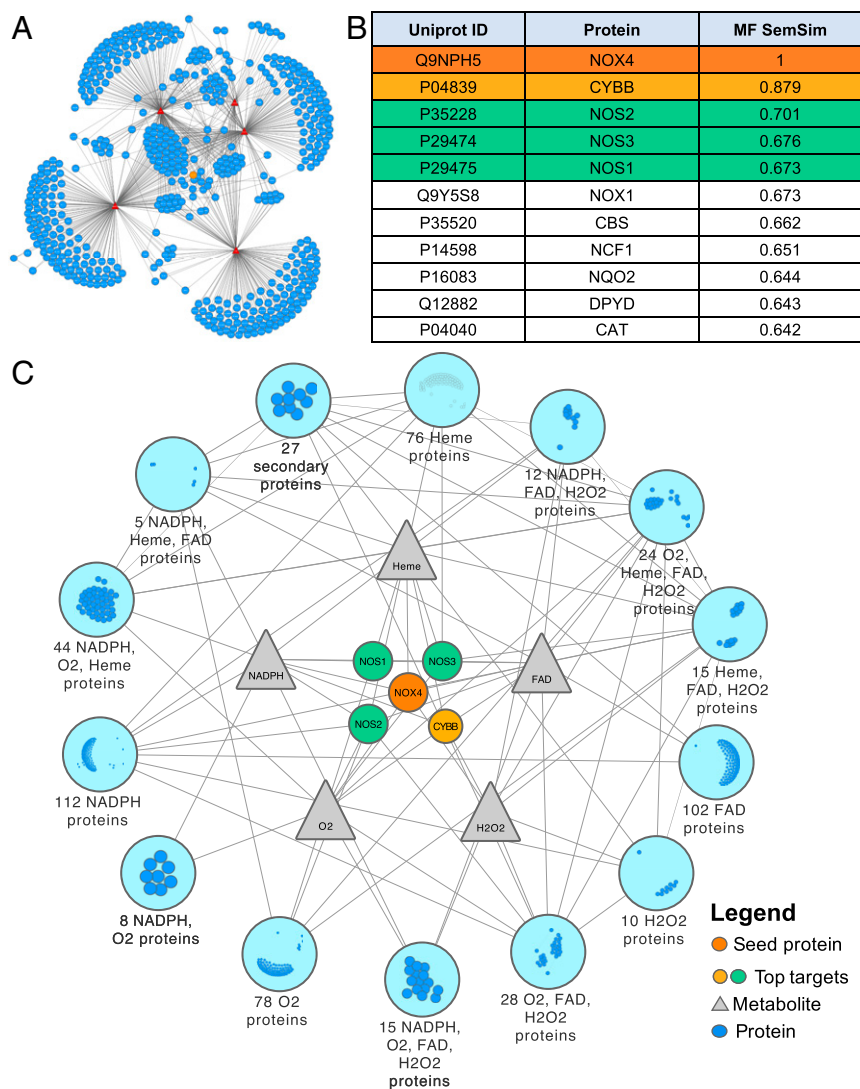
Fig. 2. Integrated NOX4-extended multilayer network of biomolecular interactions used for candidate extraction and the involved protein semantic similarity ranking. (*A*) The full network constructed using the primary protein, NOX4 (orange node), connected to its direct metabolic interactors (red nodes), which have been linked to the proteins (blue nodes) interacting with them. We also show all protein–protein and metabolite–protein interactions (gray edges). (*B*) The semantic similarity ranking based on molecular functions (MF SemSim) of proteins with the top four similar proteins is highlighted. (*C*) The simplified network with only the primary protein, and the top four similar proteins and metabolites shown individually, while the rest of the proteins are grouped as modules and their interactions are merged.

ontology (GO) molecular function annotations (22). In module 3 of our approach (Fig. 1), we computed a single score measuring the similarity of each GO term pair, which was then employed to compare the functional relatedness of two proteins. In brief, the functional relatedness score of two proteins was calculated by combining the similarity scores of every possible pair of GO terms annotating the two proteins. For scoring term pairs, we used the Wang et al. method (23) due to its ability to infer similarity according to the GO hierarchy, and not only the immediate terms in comparison. To combine these scores into the functional relatedness score of two proteins, we used the best average match strategy, as it accounts for both similar and dissimilar terms and is less affected by the number of terms available for comparison (22). Based on the assumption that functions of proteins act as a proxy for structural and biological similarity, we ranked the proteins according to their functional relatedness to NOX4 calculated based on GO similarity scores. Finally, the candidate proteins were filtered to extract the top 10 targets functionally most similar to NOX4 (Fig. 2B).

The intersection of the outcome of the semantic analysis with the list of the most connected targets from the network analysis narrowed down the candidate list of targets to only four: CYBB, NOS2, NOS3, and NOS1, which ranked as the topmost functionally similar drug targets, with similarity scores based on the molecular functions from the GO annotations of 0.87, 0.70, 0.67, and 0.67, respectively (Fig. 2 *B* and *C*). NOX1 also showed an equivalent score to NOS1; however, previous studies using a combined preclinical metaanalysis described that NOX1 plays no role in brain ischemia (24). Moreover, NOX4KO mice treated with a NOX inhibitor showed no additional effect, suggesting no additional NOX1-dependent mechanism in stroke (17). Having predicted a close connection between NOX4 and the NOS enzyme family by in silico hybrid protein–metabolic network analysis, we next wanted to validate our finding stepwise, first in vitro, then in vivo, with respect to mechanistic synergy and thus applicability for network pharmacology.

In Vitro Cotarget Validation and Drug Identification. For in vitro validation, we used two models: an organotypic hippocampal culture (OHC) and human brain microvascular endothelial cells

Table 1. Network proteins ranked according to their connectedness to NOX4 through its metabolites

Protein symbol	Protein name	UniProt ID	Connectedness to NOX4
NOS1	Nitric oxide synthase, brain	P29475	4
NOS2	Nitric oxide synthase, inducible	P35228	4
NOS3	Nitric oxide synthase, endothelial	P29474	4
HMOX1	Heme oxygenase 1	P09601	4
HMOX2	Heme oxygenase 2	P30519	4
DUOX1	Dual oxidase 1	Q9NRD9	4
DUOX2	Dual oxidase 2	Q9NRD8	4
PPOX	Protoporphyrinogen oxidase	P50336	4
AOX1	Aldehyde oxidase	Q06278	4

Proteins $n = 10$ to $n = 378$ are included in *SI Appendix*, Table S1.

as a blood–brain barrier model. In the OHC model, oxygen and glucose deprivation (OGD) followed by reoxygenation (Fig. 3*A*) resulted in the increased expression of our primary target, NOX4 (17, 18) (Fig. 3*B*), and all different NOS isoforms (Fig. 3*C*) within 2, 4, 8, 12, and 24 h post-OGD. Combinatory treatment with subthreshold concentrations of the NOX4 inhibitor GKT136901 (0.1 μM) and the NOS inhibitor L-NAME (0.3 μM) significantly reduced cell death (Fig. 3*D*) and formation of reactive

oxygen and nitrogen species 24 h post-OGD, while individual treatment with these subthreshold concentrations had no effect (Fig. 3*E*). Likewise, early kinetics (15-min) assessment of reactive oxygen species (ROS) formation postcotreatment reflected a significant reduction compared with single therapies (*SI Appendix*, Fig. S1). Similarly, in the human blood–brain barrier model, cotreatment with the same subthreshold concentrations of GKT136901 (0.1 μM) and L-NAME (0.3 μM) reduced cell death
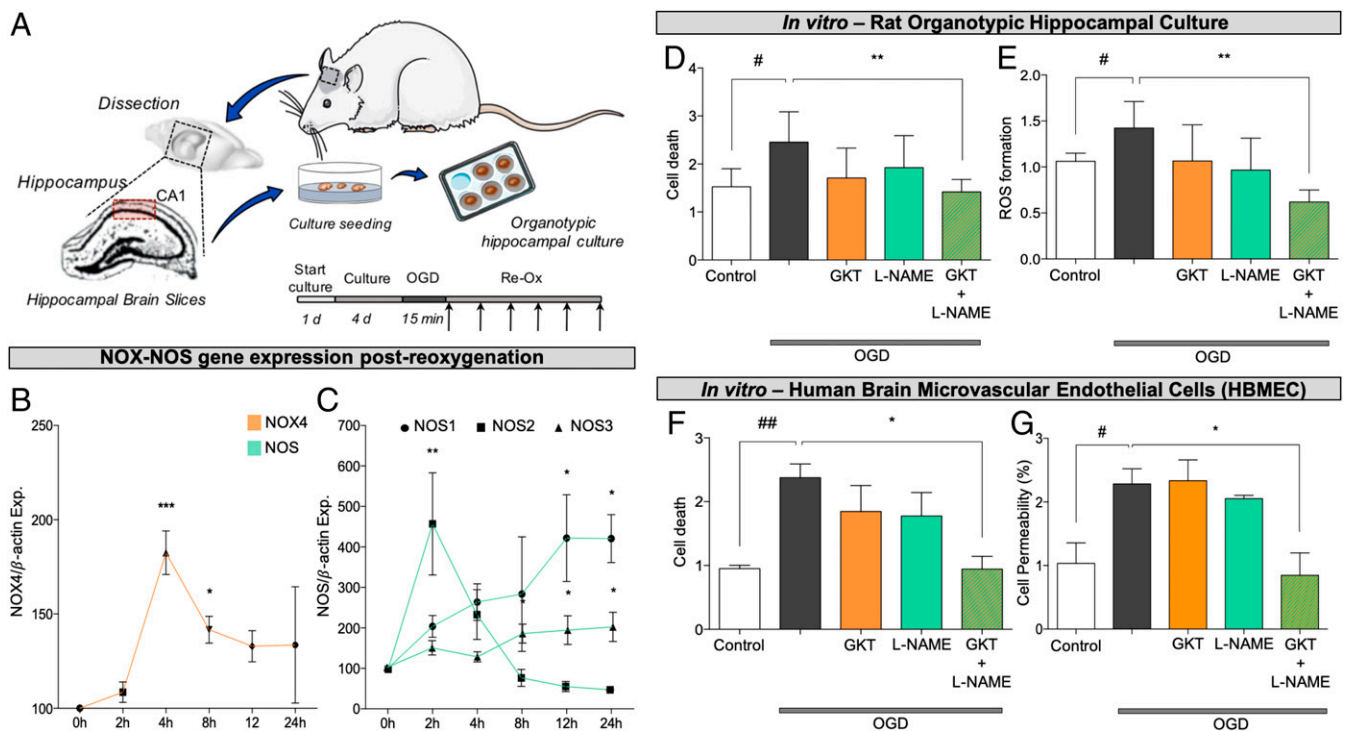

Fig. 3. In vitro cotarget validation and drug identification of NOX4 and NOS inhibitors as a combinatory treatment. (*A*) Organotypic hippocampal cultures prepared from hippocampal slices were cultured for 4 d and subsequently subjected to 15 min of OGD period followed by 24-h treatment. Samples for gene expression detection were collected at 0, 2, 4, 8, 12, and 24 h post-OGD. (*B*) NOX4 expression was up-regulated at 4 and 8 h in comparison with the beginning of the ischemia period (*$P < 0.05$, ***$P < 0.001$; $n = 3$). (*C*) Inducible NOS (NOS2; square) was up-regulated only in the first 2 h post-OGD, while neuronal NOS (NOS1; circle) was up-regulated in the final 12 to 24 h after the OGD period. Similarly, endothelial NOS (NOS3; triangle) was also significantly up-regulated at 8, 12, and 24 h post-OGD (*$P < 0.05$, **$P < 0.01$; $n = 4$). Gene expression was normalized using β-actin as housekeeping gene. (*D*) Cell death was significantly reduced in OHCs treated with GKT136901 (0.01 μM) and L-NAME (0.3 μM) in combination (**$P < 0.01$; $n = 8$; green slashed bar) in comparison with control slices (#$P < 0.05$ with respect to basal; $n = 8$; gray bar). Individual treatments show no effect. (*E*) ROS formation was also significantly decreased in OHCs treated with the combination of GKT136901 (0.01 μM) and L-NAME (0.3 μM) in comparison with nontreated slices. Again, individual treatments show no effect on cell death. #$P < 0.05$ compared with basal conditions (gray bar; $n = 5$); **$P < 0.01$ with respect to nontreated slices (gray bar; $n = 5$). (*F*) Combinatory treatment of GKT136901 and L-NAME increases cell viability in human brain microvascular endothelial cells subjected to hypoxia/reoxygenation (Re-Ox). ##$P < 0.01$ with respect to basal conditions ($n = 4$; gray bar); *$P < 0.05$ with respect to nontreated cells ($n = 4$; green slashed bar). (*G*) Cell permeability was assessed by measuring Evans blue fluorescence post-OGD. Evans blue diffusion was significantly reduced in cells treated with GKT136901 (0.01 μM) and L-NAME (0.3 μM) in combination (#$P < 0.05$; $n = 4$; gray bar) in comparison with nontreated cells (*$P < 0.05$; $n = 4$; green slashed bar). Error bars are mean ± SD.

(Fig. 3*F*) and prevented the increase in permeability after hypoxia (Fig. 3*G*). These data validated both the mechanism-based nature of NOX4 and NOS as a target and their in silico predicted synergistic interaction, since chosen monotherapies were not significantly effective.

In Vivo Validation of Network Pharmacology for Clinical Translation. To validate our network pharmacology approach in an in vivo model relevant for clinical translation, we used the mouse occlusion of the middle cerebral artery (MCAO) model in the absence or presence of GKT136901 (10 mg/kg) or L-NAME (3 mg/kg). Due to the many translational failures in stroke (25),

the Stroke Treatment Academic Industry Roundtable (STAIR) established a set of guidelines to improve the success rate. Following these STAIR criteria, we assessed both a transient and permanent model, male and female, old and young mice. First, in transient MCAO, single subthreshold treatments showed no neuroprotection (Fig. 4*A*) but combinatory treatment significantly reduced brain infarctions compared with controls (Fig. 4*A*), both at 1 h and, importantly (26), 3 h poststroke (Fig. 4*A*), suggesting a wide therapeutic time window in agreement with our in vitro expression kinetics. Similar effects in a permanent MCAO model suggested therapeutic effect independent of reperfusion (Fig. 4*A*), and thus promise for patients where
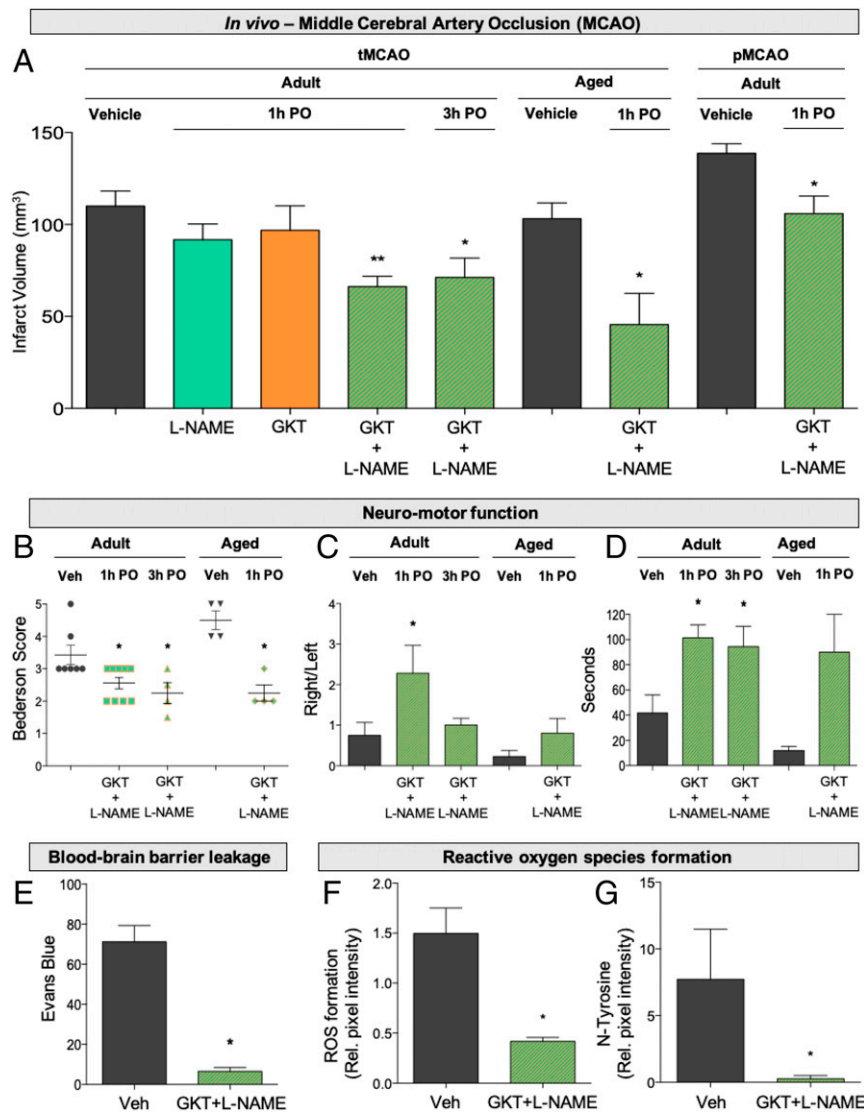
Fig. 4. In vivo validation of network pharmacology for clinical translation. (*A*) Twenty-four hours after tMCAO infarct size was reduced in mice treated with GKT136901 (10 mg/kg) and L-NAME (3 mg/kg) in combination 1 h (**P < 0.01; *n* = 6) and 3 h poststroke (*P < 0.05; *n* = 5), while individual treatment showed no effect in reduction of infarct size. Infarct volume was also significantly reduced in aged animals treated with the combination (GKT+L-NAME) 1 h poststroke (**P < 0.01; *n* = 5). Similarly, combinatory treatment decreased infarct volume after permanent occlusion of the MCA in adult mice (*P < 0.05; *n* = 5). (*B*) With respect to the neurological outcome of the combinatory treatment in surviving mice, neurological outcome (Bederson score) was improved in the adult mice treated 1 h poststroke (*P < 0.05; *n* = 9), 3 h poststroke (*P < 0.05; *n* = 5), and the aged model (*P < 0.05; *n* = 4). (*C*) Likewise, the elevated body swing test indicated a significant increase for the right swing number/total swing number ratio in adult mice treated 1 h PO (*P < 0.05; *n* = 9) but not in the other groups. (*D*) Significantly improved motor outcome was detected after four-limb hanging test in all groups: 1 h PO (*P < 0.05; *n* = 9), 3 h PO (*P < 0.05; *n* = 5), and aged animals (*P < 0.05; *n* = 4). (*E*) Blood–brain barrier integrity assessed by Evans blue extravasation was preserved in treated animals compared with nontreated mice at day 1 after 1 h of tMCAO (*P < 0.05; *n* = 4). (*F*) Treated mice showed decreased ROS formation compared with their respective nontreated animals (*P < 0.05; *n* = 4). (*G*) N-Tyr–positive cells were significantly reduced with the combinatory therapy compared with nontreated mice. (*P < 0.05; *n* = 4). Error bars are mean ± SD.

Casas et al.

www.manaraa.com

thrombolysis or/and thrombectomy is not recommended. In humans, stroke mostly occurs in the elderly population, and patient prognosis is directly influenced by age (27). Thus, we confirmed these effects in aged female and male mice (Fig. 4*A*). Although smaller infarct sizes poststroke is an important readout, neurofunctional outcome and quality of life postischemia are the main clinical parameters. Hence, we additionally assessed three independent neuromotor functioning tests in the adult mice treated 1 and 3 h poststroke together with the aged mice model: the Bederson score (Fig. 4*B*), elevated body swing test (Fig. 4*C*), and four-limb hanging wire test (Fig. 4*D*), which all were significantly improved 1 h postoperation (PO), and Bederson and the four-limb test also 3 h PO (Fig. 4 *C–E*). Monotherapies were only assessed 1 h poststroke treatment in adult mice due to ethical restrictions (*Material and Methods*). Thus, dual NOX/ NOS inhibition poststroke leads to a potent synergistic, mechanism-based, and neuroprotective effect, further confirming that both targets are causally linked in a clinically translatable manner.

Prevention of Blood–Brain Barrier Disruption and ROS Formation upon Stroke Treatment. The cerebral vasculature, which is critical for the maintenance of the blood–brain barrier (BBB), is particularly susceptible to oxidative stress (28, 29). To test whether dual inhibition of NOX/NOS leads to the blood–brain barrier phenotype, we assessed the integrity of the blood–brain barrier after ischemic stroke. In line with previous findings, combinatory treatment significantly reduced blood–brain barrier disruption upon stroke compared with nontreated mice (Fig. 4*E*).

To link the neuroprotective effect on the enzymatic activity of both ROS sources, we measured oxidative stress and N-Tyr formation in brain tissue cryosections. ROS generation and N-Tyr formation were dramatically reduced in treated mice (Fig. 4*F*) after 24 h of cotreatment (Fig. 4*G*), demonstrating a direct link in ROS reduction and a broad neuroprotective effect (*SI Appendix*, Figs. S2 and S3).

Discussion

We here report a proof of concept for an in silico discovery approach to pair a single validated therapeutic drug target with another mechanistically related one for synergistic network pharmacology. Our multilayered interactome analysis including metabolites coupled with semantic similarity ranking detects pathomechanistically related proteins which can be cotargeted. Using this approach, we extend NOX4 to the closest functional neighbor gene, NOS.

In search for a secondary, synergistic, and causal network pharmacology target prediction, data-driven or modeling-based techniques have been developed. A data-driven approach integrated multiple sources of data on drugs such as target proteins and their pathways, medical indications, therapeutic effects, and side effects (30). DrugComboRanker prioritizes synergistic drug combinations (31) by constructing a functional drug network, although restricted to cancer drug–gene profiles. Here, community detection is performed via Bayesian non-negative matrix factorization and, finally, similar drugs are inferred based on an adjacency matrix built from the drug–target network.

With respect to modeling, a network-based approach ranked combinations of proteins using a topological score calculated from an integrated protein–protein interaction (PPI) network constructed and enriched with gene expression data from a singular disease phenotype (13). Random forests were used to predict drug combinations by exploiting network features generated from PPI data, and drug chemical and pharmacogenomic features from drug-induced expression profiles (11). MASCOT is a model-driven machine-learning algorithm that leverages curated dynamic models of signaling networks and their disease states to predict synergistic targets of a desired therapeutic effect

(14). In comparison with all these previous reports, our two-step approach utilized experimental databases on multilevel molecular networks in a rather simple and generic manner, and our predictions were experimentally validated both in vitro and in vivo.

PPI networks or interactomes have been commonly used to understand complex disease mechanisms (32–36). However, PPI networks are just one level of molecular interaction networks. Most signaling events are not due to wild-type PPIs but involve metabolites or metabolic protein modifications. We therefore used protein–metabolite networks in conjunction with PPI networks. In addition, this solved another issue of molecular interaction databases. Current databases suffer from selection and detection biases, high rates of false positives, and low rates of coverage (5, 37).

However, metabolome databases still have severe shortcomings. When querying the most comprehensive HMDB with seven additional key signaling enzymes, key metabolites were consistently missing, namely for soluble guanylate cyclase, the substrate, GTP, and the product, 2′,5′-cGMP, as well as GMP, cAMP, and 2′,3′-cGMP being wrongly listed. Thus, our approach will improve considerably once these or other metabolic databases are intensely curated and become more complete.

Although our method is generic and can be applied to other cases in concept, there are restrictions. For instance, the current computational pipeline supports one seed target; however, it is generally applicable to more than one seed target. For multiple seed targets, one would have to look for druggable candidates with the shortest average distance in the graph representation of the integrated network to all seeds.

In the network analysis step, the patchiness of the data sources may affect predictions, while for the semantic similarity, the availability and accuracy of GO annotations may impact on the ranking. In addition, we report only a single validated application of our method, and further use cases will be needed. In fact, NOX4-related targets, namely NCF1, NQO2, and DPYD, might also show potential. Targeting NCF1, also known as p47 (NOX subunit), may lead to indirect NOX4 activation. However, modulating NCF1 is so far not possible, since protein–protein interaction inhibitors proved noneffective and no further network pharmacology strategy could be achieved (38). Moreover, ribosyl dihydronicotinamide dehydrogenase (NQO2), a ROS-generating enzyme, shows a direct acetaminophen side effect, while this drug has been shown as protective in stroke, demonstrating a direct link (39). However, when weighing NQO2 and NOS as a cotarget of NOX4, we would still prefer NOS, because with NOX4 and NQO2 we would both target ROS formation with possibly no synergy but rather additive effects.

We thus validated the therapeutic applicability of our in silico network pharmacology hypothesis both in vitro and in vivo by coadministering both a NOX inhibitor and NOS inhibitor, respectively, in three different species including a human BBB model. Of high translational relevance, combining a NOX and NOS inhibitor conveyed in direct neuroprotection in three different brain ischemia models, rat organotypic hippocampal culture, transient and permanent MCAO in mice, and human brain microvascular cells as a BBB model. Importantly, this was achieved at concentrations and doses, respectively, that on their own were ineffective. This will allow extension of the clinical translation of NOX4 inhibition in stroke to be enhanced in efficacy and safety by lowering in risk of any potential side effects, increasing mechanistic-based synergy and reducing the number needed to treat. Thus, our multitargeted approach therefore focuses on NOX4 inhibition coadministered with a NOS inhibitor while, due to synergy, reducing the doses/concentrations of both drugs to individual subthreshold levels.

On a mechanistic level, interaction between reactive oxygen species and NO, for example, to toxify NO via intermediate

www.manaraa.com

peroxynitrite formation, has been shown before (40). The source of ROS, however, has not always been identified (41–43). Also, the signaling networks of NOS/NO on the one side and ROS formation and ROS targets on the other have been annotated as rather independent. Here, we show that, at least in disease, both networks represent subnetworks of the same common mechanism that involves both NOS and NOX4. At least NOX4 is one relevant ROS source interacting with NO, or NO's downstream signaling and online pathways have been suggested for curation, as far as possible. Importantly, this does not imply that all ROS sources will interact as well with NOS. Such assumptions represent a shortcoming of the current curated NOS and ROS pathways, as they combine, for example, all ROS sources and all ROS targets into one scheme. With respect to the relevant NOS isoform, the best characterized and validated is NOS1 (44), whereas NOS3 is rather protective (45) and NOS2 expression commences only 12 h after the onset of the stroke in an in vivo rat model (46), while our findings suggest different expression in mice primarily due to model and species differences.

With respect to clinical application there are two other NOS inhibitors worth being considered apart from L-NAME, which has been tested for the longest time. First, Vasopharm is developing VAS203 as a NOS common inhibitor currently entering phase III clinical trials for traumatic brain injury. Since it is a NOS common inhibitor like L-NAME it has a similar spectrum, but concerns have arisen with respect to covalent off-target effects (47, 48) and depression of kidney function (49). Second, S-methyl-L-thiocitrulline has also been tested in humans but appears to have only a limited spectrum, possibly limited to NOS1 (1), while our in silico prediction ranked NOS2 > NOS3 > NOS1. Such isoform-selective inhibitors will certainly be of interest in future studies aiming at deciphering the contribution of individual NOS isoforms in ROS–NO interaction.

Clearly, more de novo generated pathways as subgraphs of the interactome are necessary to eliminate such assumptions. Also, NOX4 generates H_2O_2, whereas typically superoxide, O_2^-, is considered the key interfering molecule with respect to NO. Moreover, NOX4 has also been identified as a positive indirect transcriptional regulator of the major H_2S-producing enzyme, cystathionine β-synthase (50), which plays a key role in the central nervous system and circulation linked to worse poststroke outcome (51). Thus, poststroke NOX4-dependent inhibition of the cystathionine β-synthase pathway may also result in at least additive effective effects in stroke within the same mechanistic network.

With respect to NOS1 to 3, the possibility exists that one of the isoforms may actually be protective. Importantly, the here-presented network approaches are by definition undirected, namely whether a cotarget needs to be inhibited or activated is not always immediately obvious. Chronically, NOS3 inhibition is certainly not of benefit (11); however, in an acute setting, even endothelial NOS-derived NO may for a time window where it interacts with NOX4-derived ROS be detrimental. Pan-NOS inhibition is almost as effective as NOS1 knockout. Thus, pharmacological validation will in many cases remain an essential component when interpreting and curating network pharmacology discovery results.

Thus, from a chemical point of view, the NOX4–NOS interaction that we predicted and validated was surprising, and may involve a hitherto underappreciated interaction of H_2O_2 with transition metal centers to form singlet oxygen (40, 52).

In conclusion, our present and other network pharmacology approaches (1, 53) provide a roadmap to reduce the risk of failure in single drug target development by moving toward multiple targeting of de novo causal networks to increase therapeutic efficacy and reduce individual drug dosing and possible side effects due to mechanism-based synergy (53, 54). We suggest extending our approach to other unmet medical need indications, where currently only single drug- or symptom-based approaches are available.

Material and Methods

Detailed experimental procedures are provided in *SI Appendix, Material and Methods*.

Study Design. All animal experiments were performed after approval of the protocol by the Institutional Ethics Committee of the Autonomous University of Madrid according to European guidelines for the use and care of animals for research. The dropout rates were four mice in the vehicle groups [transient (t)MCAO, aged, permanent (p)MCAO, and Evans blue] versus three mice in different treatment groups (tMCAO and pMCAO) (*SI Appendix*, Table S2). Post hoc power analysis for adult mice is included in *SI Appendix*, Table S3.

Transient Occlusion of the Middle Cerebral Artery. The model was previously described in ref. 17.

Human Brain Microvascular Endothelial Cells Subjected to Hypoxia. Human brain microvascular endothelial cells (HBMECs) (Cell Systems) were cultured to ~90% confluence. Cell medium was replaced by non–FBS-containing medium (2 mL per well) following 6 h of hypoxia (94.8% N_2, 0.2% O_2, and 5% CO_2) and 24 h of reperfusion in the presence or absence of the pharmacological treatment (see *SI Appendix* for details).

Statistical Analysis. All results obtained from the in vitro (hippocampal brain slices, OHCs, HBMECs) and in vivo (tMCAO) ischemia models were analyzed using Prism 5.0 software (GraphPad Software). Data were expressed as the means ± SEM of separate experiments. Statistical comparisons between groups were performed using one-way ANOVA, followed by a Newman–Keuls multiple-comparison test. Differences between two groups were considered significant at $P < 0.05$. Numbers of animals necessary to detect a standardized effect size on infarct volumes ≥0.2 (vehicle-treated control mice vs. treated mice) were determined via a priori sample size calculation with the following assumptions: $\alpha = 0.05$; $\beta = 0.2$; 20% SD of the mean. In each case, when only two groups were compared, the unpaired two-tailed Student's t test was applied followed by a Mann–Whitney U test, where significance was considered at $P < 0.05$.

1. Yildirim MA, Goh K-I, Cusick ME, Barabási A-L, Vidal M (2007) Drug-target network. *Nat Biotechnol* 25:1119–1126.
2. Aguirre-Plans J, et al. (2018) Proximal pathway enrichment analysis for targeting comorbid diseases via network endopharmacology. *Pharmaceuticals (Basel)* 11:E61.
3. Hopkins AL (2007) Network pharmacology. *Nat Biotechnol* 25:1110–1111.
4. Scannell JW, Blanckley A, Boldon H, Warrington B (2012) Diagnosing the decline in pharmaceutical R&D efficiency. *Nat Rev Drug Discov* 11:191–200.
5. Menche J, et al. (2015) Disease networks. Uncovering disease-disease relationships through the incomplete interactome. *Science* 347:1257601.
6. Langhauser F, et al. (2018) A diseasome cluster-based drug repurposing of soluble guanylate cyclase activators from smooth muscle relaxation to direct neuroprotection. *NPJ Syst Biol Appl* 4:8.
7. Barabási A-L, Oltvai ZN (2004) Network biology: Understanding the cell's functional organization. *Nat Rev Genet* 5:101–113.
8. Batra R, et al. (2017) On the performance of de novo pathway enrichment. *NPJ Syst Biol Appl* 3:6.
9. Alcaraz N, et al. (2017) De novo pathway-based biomarker identification. *Nucleic Acids Res* 45:e151.
10. Koduru P, Chaganti R (1988) Congenital chromosome breakage clusters within Giemsa-light bands and identifies sites of chromatin instability. *Cytogenet Cell Genet* 49:269–274.
11. Li X, et al. (2017) Prediction of synergistic anti-cancer drug combinations based on drug target network and drug induced gene expression profiles. *Artif Intell Med* 83:35–43.
12. Meladze VG (1985) [Temporal characteristics of the autoregulation process of local cerebral blood flow in hypo- and hypertension]. *Patol Fiziol Eksp Ter,* 29–32. Russian.
13. Vitali F, Mulas F, Marini P, Bellazzi R (2013) Network-based target ranking for polypharmacological therapies. *J Biomed Inform* 46:876–881.

Casas et al.

14. Chua HE, Bhowmick SS, Tucker-Kellogg L (2017) Synergistic target combination prediction from curated signaling networks: Machine learning meets systems biology and pharmacology. *Methods* 129:60–80.

15. Vilar S, Hripcsak G (2017) The role of drug profiles as similarity metrics: Applications to repurposing, adverse effects detection and drug-drug interactions. *Brief Bioinform* 18:670–681.

16. Guney E (2017) Reproducible drug repurposing: When similarity does not suffice. *Pac Symp Biocomput* 22:132–143.

17. Casas AI, et al. (2017) NOX4-dependent neuronal autotoxicity and BBB breakdown explain the superior sensitivity of the brain to ischemic damage. *Proc Natl Acad Sci USA* 114:12315–12320.

18. Kleinschnitz C, et al. (2010) Post-stroke inhibition of induced NADPH oxidase type 4 prevents oxidative stress and neurodegeneration. *PLoS Biol* 8:e1000479.

19. Li F, Xu W, Zhao S (2013) Regulatory roles of metabolites in cell signaling networks. *J Genet Genomics* 40:367–374.

20. Nisimoto Y, Diebold BA, Cosentino-Gomes D, Lambeth JD (2014) Nox4: A hydrogen peroxide-generating oxygen sensor. *Biochemistry* 53:5111–5120, and erratum (2014) 53:5472.

21. Piovesan D, Giollo M, Ferrari C, Tosatto SCE (2015) Protein function prediction using guilty by association from interaction networks. *Amino Acids* 47:2583–2592.

22. Pesquita C, et al. (2008) Metrics for GO based protein semantic similarity: A systematic evaluation. *BMC Bioinformatics* 9(Suppl 5):S4.

23. Wang JZ, Du Z, Payattakool R, Yu PS, Chen C-F (2007) A new method to measure the semantic similarity of GO terms. *Bioinformatics* 23:1274–1281.

24. Kleikers PWM, et al. (2015) A combined pre-clinical meta-analysis and randomized confirmatory trial approach to improve data validity for therapeutic target validation. *Sci Rep* 5:13428.

25. O'Collins VE, et al. (2006) 1,026 experimental treatments in acute stroke. *Ann Neurol* 59:467–477.

26. Peña ID, Borlongan C, Shen G, Davis W (2017) Strategies to extend thrombolytic time window for ischemic stroke treatment: An unmet clinical need. *J Stroke* 19:50–60.

27. Chen R-L, Balami JS, Esiri MM, Chen L-K, Buchan AM (2010) Ischemic stroke in the elderly: An overview of evidence. *Nat Rev Neurol* 6:256–265.

28. Lehner C, et al. (2011) Oxidative stress and blood-brain barrier dysfunction under particular consideration of matrix metalloproteinases. *Antioxid Redox Signal* 15:1305–1323.

29. Enciu A-M, Gherghiceanu M, Popescu BO (2013) Triggers and effectors of oxidative stress at blood-brain barrier level: Relevance for brain ageing and neurodegeneration. *Oxid Med Cell Longev* 2013:297512.

30. Zhao X-M, et al. (2011) Prediction of drug combinations by integrating molecular and pharmacological data. *PLoS Comput Biol* 7:e1002323.

31. Huang L, et al. (2014) DrugComboRanker: Drug combination discovery based on target network analysis. *Bioinformatics* 30:i228–i236.

32. Vidal M, Cusick ME, Barabási A-L (2011) Interactome networks and human disease. *Cell* 144:986–998.

33. Futschik ME, Chaurasia G, Herzel H (2007) Comparison of human protein-protein interaction maps. *Bioinformatics* 23:605–611.

34. Lehne B, Schlitt T (2009) Protein-protein interaction databases: Keeping up with growing interactomes. *Hum Genomics* 3:291–297.

35. Rolland T, et al. (2014) A proteome-scale map of the human interactome network. *Cell* 159:1212–1226.

36. Mehta V, Trinkle-Mulcahy L (2016) Recent advances in large-scale protein interactome mapping. *F1000 Res* 5:782.

37. Amaral LAN (2008) A truer measure of our ignorance. *Proc Natl Acad Sci USA* 105:6795–6796.

38. Altenhöfer S, Radermacher KA, Kleikers PWM, Wingler K, Schmidt HHHW (2015) Evolution of NADPH oxidase inhibitors: Selectivity and mechanisms for target engagement. *Antioxid Redox Signal* 23:406–427.

39. Miettinen TP, Björklund M (2014) NQO2 is a reactive oxygen species generating off-target for acetaminophen. *Mol Pharm* 11:4395–4404.

40. Radi R (2018) Oxygen radicals, nitric oxide, and peroxynitrite: Redox pathways in molecular medicine. *Proc Natl Acad Sci USA* 115:5839–5848.

41. Geiszt M (2006) NADPH oxidases: New kids on the block. *Cardiovasc Res* 71:289–299.

42. Espey MG, et al. (2002) A chemical perspective on the interplay between NO, reactive oxygen species, and reactive nitrogen oxide species. *Ann N Y Acad Sci* 962:195–206.

43. Ghezzi P, Jaquet V, Marcucci F, Schmidt HHHW (2017) The oxidative stress theory of disease: Levels of evidence and epistemological aspects. *Br J Pharmacol* 174:1784–1796.

44. Kleinschnitz C, et al. (2016) NOS knockout or inhibition but not disrupting PSD-95-NOS interaction protect against ischemic brain damage. *J Cereb Blood Flow Metab* 36:1508–1512.

45. Endres M, Laufs U, Liao JK, Moskowitz MA (2004) Targeting eNOS for stroke protection. *Trends Neurosci* 27:283–289.

46. Niwa M, et al. (2001) Time course of expression of three nitric oxide synthase isoforms after transient middle cerebral artery occlusion in rats. *Neurol Med Chir (Tokyo)* 41:63–73.

47. Dao VT-V, et al. (2015) Pharmacology and clinical drug candidates in redox medicine. *Antioxid Redox Signal* 23:1113–1129.

48. Sun Q-A, Hess DT, Wang B, Miyagi M, Stamler JS (2012) Off-target thiol alkylation by the NADPH oxidase inhibitor 3-benzyl-7-(2-benzoxazolyl)thio-1,2,3-triazolo[4,5-d]pyrimidine (VAS2870). *Free Radic Biol Med* 52:1897–1902.

49. Ott C, et al. (January 21, 2019) Effects of the nitric oxide synthase inhibitor ronopterin (VAS203) on renal function in healthy volunteers. *Br J Clin Pharmacol*, 10.1111/bcp.13870.

50. Mistry RK, et al. (2016) Transcriptional regulation of cystathionine-γ-lyase in endothelial cells by NADPH oxidase 4-dependent signaling. *J Biol Chem* 291:1774–1788.

51. Chan SJ, et al. (2015) Cystathionine β-synthase inhibition is a potential therapeutic approach to treatment of ischemic injury. *ASN Neuro* 7:1759091415578711.

52. Noronha-Dutra AA, Epperlein MM, Woolf N (1993) Reaction of nitric oxide with hydrogen peroxide to produce potentially cytotoxic singlet oxygen as a model for nitric oxide-mediated killing. *FEBS Lett* 321:59–62.

53. Hopkins AL (2008) Network pharmacology: The next paradigm in drug discovery. *Nat Chem Biol* 4:682–690.

54. Tang J, Aittokallio T (2014) Network pharmacology strategies toward multi-target anticancer therapies: From computational models to experimental design principles. *Curr Pharm Des* 20:23–36.